INT. J. REMOTE SENSING, 1997, VOL. 18, NO. 18, 3883–3888

Detection of changes in remotely-sensed images by the selective use of multi-spectral information

L. BRUZZONE and S. B. SERPICO

Department of Biophysical and Electronic Engineering, University of Genoa, Via Opera Pia, 11a, I-16145 Genova, Italy

(*Received 8 January 1997; in final form 23 May 1997*)

Abstract. In this Letter, an unsupervised algorithm for detecting changes in multi-spectral and multi-temporal remotely-sensed images is presented. Such an algorithm makes it possible to reduce the effects of 'registration noise' on the accuracy of change detection. In addition, it can be used to reduce the typologies of detected changes in order to better locate the changes under investigation.

1. Introduction

Detection of land-cover changes, by comparing the images acquired in the same area at different times, is one of the major applications of remotely-sensed images acquired by Earth-orbiting satellites (Singh 1989).

One of the most widely used change-detection techniques is univariate image differencing (UID) (Singh 1989, Fung 1990). Two spatially registered images acquired at two different times are subtracted on a pixel basis to produce a further image (difference image) which represents the changes between the two. Under the hypothesis of few changes between the two times, changes can be detected in the tails of the statistical distribution of the pixel values in the difference image.

The above technique is usually applied by using a spectral band where the typologies of investigated changes can be detected. However, other typologies of non-investigated changes are often detected, too. In particular, a typology of false changes due to image misalignments is often detected (registration noise) (Gong *et al.* 1992, Townshend *et al.* 1992).

In this Letter, we present a new algorithm which allows a selective detection of land-cover changes by exploiting the information available in multi-spectral remotely-sensed images. In particular, this algorithm is useful to reduce the effects of registration noise.

2. The proposed approach

In remote sensing applications, we are often interested in detecting only a specific kind of land-cover change. Each kind of land-cover change can usually be well detected only in a subset of multi-temporal spectral bands, while it is not detectable in other bands. In the proposed algorithm, we utilize not only the bands where the investigated change is detectable but also other bands where it is not detectable. In particular, we employ the latter bands to identify pixels affected by registration noise and pixels belonging to other non-investigated changes. Then this information is used to reduce such 'disturbing effects' in the spectral bands where the investigated change is visible and, consequently, in the final map of changes. In the following,

0143–1161/97 $12.00 © 1997 Taylor & Francis Ltd

this algorithm is indicated by the acronym 'SMI', which stands for 'Selective use of Multi-spectral Information'.

2.1. *SMI algorithm*

Let $B^{t_1}=\{b_1^{t_1}, b_2^{t_1}, \dots, b_N^{t_1}\}$ and $B^{t_2}=\{b_1^{t_2}, b_2^{t_2}, \dots, b_N^{t_2}\}$ be the sets of N spectral bands of images acquired at time t_1 and t_2, respectively. Let C_i be the set of typologies of changes detectable by comparing $b_i^{t_1}$ with $b_i^{t_2}$ ($i=1, \dots, N$), c^* the typology of the investigated change, and c^{reg} the typology related to false changes due to registration noise.

step 1: select two spectral bands, b_h and b_k, such that $c^* \in C_h$, $c^* \notin C_k$, $c^{\text{reg}} \in C_h$, and $c^{\text{reg}} \in C_k$. (It is worth noting that usually $c^{\text{reg}} \in C_i$, $i=1, \dots, N$, as registration noise is generally visible in all spectral bands.)

step 2: for each pair of pixels with the same co-ordinates (i, j) in the two multitemporal images, compute the following differences:

$$D_h(i, j)=b_h^{t_2}(i, j)-b_h^{t_1}(i, j) \tag{1}$$

$$D_k(i, j)=b_k^{t_2}(i, j)-b_k^{t_1}(i, j) \tag{2}$$

The difference images D_h and D_k provide information on the sets of changes C_h and C_k, respectively.

step 3: to make D_h and D_k directly comparable, replace the value of each pixel with the Mahalanobis distance (Richards 1993) of the value of such a pixel from the distribution of the related difference image, i.e.,

$$D_h'(i, j)=\sqrt{\frac{[D_h(i, j)-\bar{D}_h]^2}{\sigma_{D_h}^2}} \qquad D_k'(i, j)=\sqrt{\frac{[D_k(i, j)-\bar{D}_k]^2}{\sigma_{D_k}^2}} \tag{3}$$

where $\bar{D}_h$, $\bar{D}_k$, $\sigma_{D_h}^2$, and $\sigma_{D_k}^2$ are the averages and the variances of the distributions of the values of the pixels in D_h and D_k which are considered to be Gaussian, as in the UID technique for the case of a small number of changed pixels. D_h' and D_k' take only positive values.

step 4: for each pair of spatially corresponding pixels compute the following difference:

$$D_{hk}(i, j)=D_h'(i, j)-D_k'(i, j) \tag{4}$$

step 5: compute the mean value $\bar{D}_{hk}$ and the variance $\sigma_{D_{hk}}^2$ of D_{hk}. Pixels with typologies of changes belonging to C_h but not to C_k (i.e., belonging to $[C_h-(C_h \cap C_k)]$) take on values that are in the positive tail of such a distribution; no-change pixels and pixels with typologies of changes belonging to both C_h and C_k (i.e., belonging to $C_h \cap C_k$) (including false changes due to registration noise) are grouped around the mean value; pixels with typologies of changes belonging to C_k but not to C_h (i.e., belonging to $[C_k-(C_h \cap C_k)]$) are in the negative tail of the distribution. Since $c^* \in [C_h-(C_h \cap C_k)]$, then the investigated change can be detected by the following condition:

$$D_{hk}(i, j)>\bar{D}_{hk}+t\sigma_{D_{hk}} \tag{5}$$

where a suitable value of the constant t can be found by experiments. Also for the SMI algorithm, as for the UID technique, it is necessary to find a value of t that assures a good trade-off between the amount of false detections and missed changes.

If the set of detected changes $[C_h - (C_h \cap C_k)]$ contains only c^*, then the SMI algorithm allows one to reveal c^* alone; otherwise, also the other changes in $[C_h - (C_h \cap C_k)]$ (i.e., all the changes that are visible in b_h but not in b_k) are revealed in the final map.

In the latter case, a further focalization of c^* can be obtained by further applications of the SMI algorithm. For example, if there exists a band b_j in which all changes revealed at the first application of the algorithm but c^* are detectable, then c^* can be isolated by applying the algorithm again, using b_j in place of b_k. The *AND* of the binary maps resulting from the two applications of the algorithm provides a final map which highlights only pixels belonging to the typology of the investigated change c^* (in a ideal situation with no errors).

3. Experimental results

The study region is a mountainous area in northern Italy, near Lake Garda. A section of two multi-spectral images (600 pixels by 600 pixels) acquired by the Thematic Mapper (TM) sensor in February 1992 and March 1993 (figure 1), respectively, was used. Four forest fires occurred between the two dates in the selected area (figure 1). In addition, other changes due to the extension of areas covered with

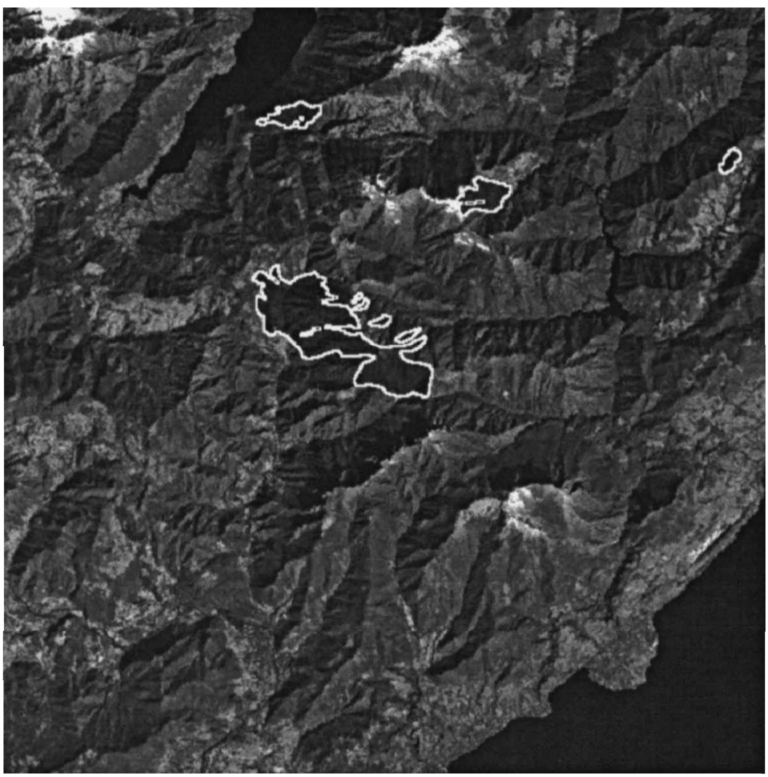

Figure 1. Section (600 pixels by 600 pixels) of band 4 of a multi-spectral image acquired by the Landsat TM sensor in March 1993 on a mountainous area in northern Italy (burned areas are indicated).

snow occurred. The SMI algorithm was used to detect just burned areas. To validate the algorithm, the obtained results were compared with the ones provided by the standard UID technique.

The two multi-spectral images were registered with an accuracy of less than one pixel. Then they were preprocessed to reduce the differences in illumination related to the two acquisition times by applying a histogram matching technique (Chavez and Mackinnon 1994). This is a crucial task since differences in illumination may be erroneously interpreted by the change-detection algorithms as land-cover changes (Olsson 1993).

According to the SMI algorithm, band 4 of the TM sensor was selected as b_h, as it was the best one to detect burned areas; band 7 was used as b_k in order to reduce the effects of registration noise, as in our images burned areas were not detectable in band 7. Furthermore, burned areas were not detectable in band 1, whereas areas covered with snow were easily detected in it. Therefore, the algorithm was applied again by using band 1 as b_j in order to reduce the effects of changes in areas covered with snow. The UID technique was applied by using band 4 of TM.

We selected values of the threshold t in order to obtain an equal number of missed pixels in burned areas for both the SMI and the UID algorithms; then, we compared the results on the basis of the false indications of changes they provided. For this purpose, we selected the pair of values $t = 1{\cdot}3$ for SMI and $t = 2{\cdot}0$ for UID as a good compromise between false and missed changes since the amount of missed

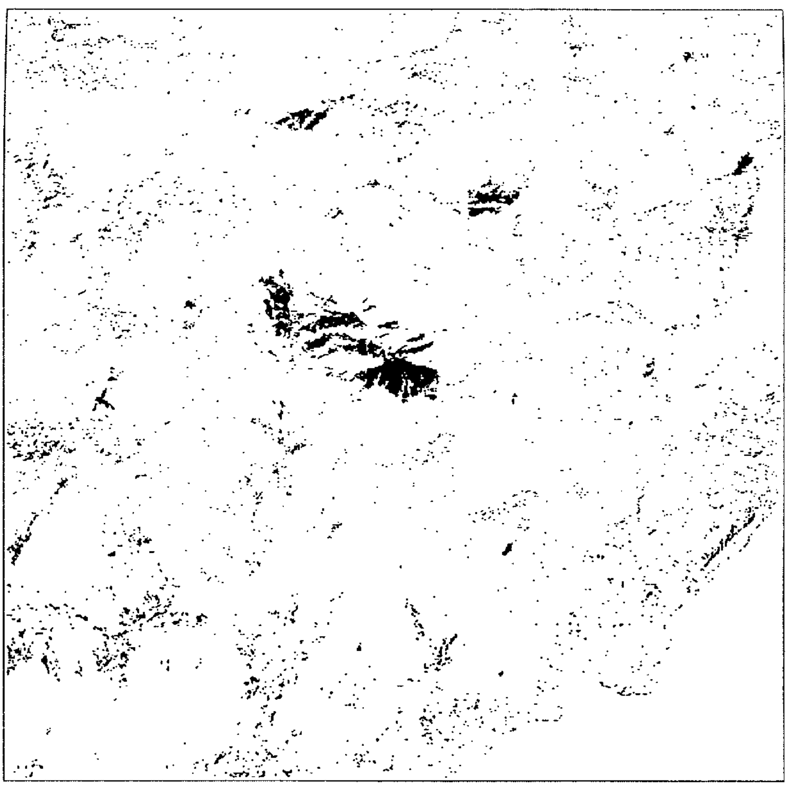

Figure 2. Map of changes provided by the proposed algorithm: 3710 pixels are missed in burned areas, 6032 pixels of false changes are detected in other areas.

pixels (i.e., 3710 for both the algorithms) still allowed the four forest fires to be located with reasonable accuracy. In this situation, the performances of SMI were remarkably higher, since it provided 6032 pixels of false changes (figure 2) with respect to 13 265 pixels of false changes provided by UID (figure 3). In particular, the reduction in false changes due to registration noise is clearly visible, for instance, on the shores of the lake in the upper left and lower right parts of the image. The strong reduction in the detection of non-investigated changes due to areas covered with snow is also visible (see, for example, the upper-left and middle parts of the image).

Most of the false changes in the map produced by SMI (figure 2) can be easily removed by applying image-filtering algorithms (Richards 1993), since they consist mainly of isolated points. On the contrary, in the map provided by the UID (figure 3) there are several false change areas that cannot be removed because they have features that are similar to those of the areas of investigated changes (i.e., forest fires).

4. Conclusions

In this Letter, we have proposed a new change-detection algorithm which allows a selective detection of land-cover changes by exploiting the information available in multi-spectral remotely-sensed images. In particular, the proposed algorithm also

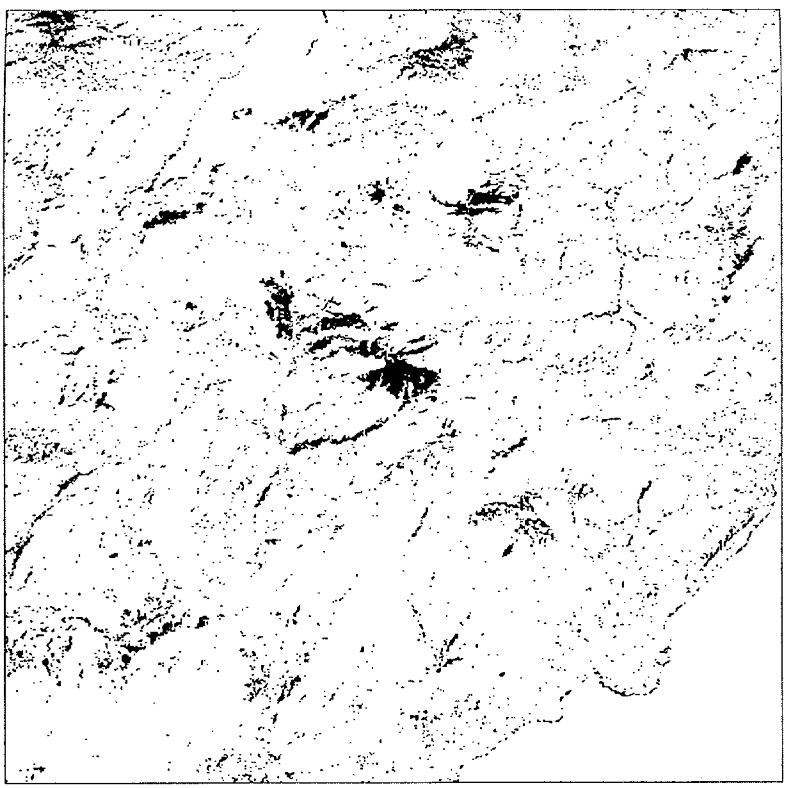

Figure 3. Map of changes provided by the univariate image differencing technique: 3710 pixels are missed in burned areas, 13 625 pixels of false changes are detected in other areas.

utilizes the spectral bands where investigated changes are not visible in order to reduce the registration noise and the effects of non-investigated changes.

An experiment with real data has been presented. The results we obtained and the favourable comparison with the standard UID technique confirm the interest of our algorithm.

It is worth noting that the selected study area, being a mountainous zone, is quite a complex test region. In fact, illumination and nadir location differences between multitemporal images may produce a higher amount of non-investigated changes than those produced on flat areas.

Acknowledgments

This research was conducted within the framework of the research project 'Integrated assessment of environmental degradation connected with forest fires in European areas', which was funded by the European Commission (Environment Programme II, Contract N. EV5V-CT94-0481). This support is gratefully acknowledged.

The authors wish to thank Dr E. Binaghi and Dr A. Rampini (C.N.R.-I.T.I.M., Milan, Italy) for providing the TM images, and the anonymous referees for their constructive criticisms.

References

Chavez, P. S. Jr., and Mackinnon, D. J., 1994, Automatic detection of vegetation changes in the southwestern United States using remotely-sensed images. *Photogrammetric Engineering & Remote Sensing*, **60,** 571–583.

Fung, T., 1990, An assessment of TM imagery for land-cover change detection. *I.E.E.E. Transactions on Geoscience and Remote Sensing*, **28,** 681–684.

Gong, P., Ledrew, E. F., and Miller, J. R., 1992, Registration-noise reduction in difference images for change detection. *International Journal of Remote Sensing*, **13,** 773–779.

Olsson, H., 1993, Regression functions for multitemporal relative calibration of thematic mapper data over boreal forest. *Remote Sensing of Environment*, **46,** 89–102.

Richards, J. A., 1993, *Remote Sensing Digital Image Analysis*, 2nd edn (London: Springer-Verlag).

Singh, A., 1989, Digital change detection techniques using remotely-sensed data. *International Journal of Remote Sensing*, **10,** 989–1003.

Townshend, J. R. G., Justice, C. O., and Gurney, C., 1992, The impact of misregistration on change detection. *I.E.E.E. Transactions on Geoscience and Remote Sensing*, **30,** 1054–1060.